ASEAN
Journal of Scientific and Technological Reports
Online ISSN:2773-8752

Research article

Enhanced Thermal Efficiency of Solar Air Heaters Using Porous Material: An Experimental Approach

Eakpoom Boonthum[1], Prapanphong Somsila[2], Apinunt Namkhat[1], Sorawit Sonsaree[3], and Umphisak Teeboonma[1*]

[1] Faculty of Engineering, Ubon Ratchathani University, Ubon Ratchathani, 34190, Thailand
[2] Faculty of Agriculture and Technology, Rajamangala University of Technology Isan, Surin Campus, Surin, 32000, Thailand
[3] Faculty of Industrial Technology, Pibulsongkram Rajabhat University, Phitsanulok, 65000, Thailand
* Correspondence: umphisak.t@ubu.ac.th

Citation:
Boonthum, E.; Somsila, P.; Namkhet, A.; Sonsaree, S.; Teeboonma, U. Enhanced thermal efficiency of solar air heaters using porous materials: an experimental approach. *ASEAN J. Sci. Tech. Report.* **2026**, *29*(1), e259025. https://doi.org/10.55164/ajstr.v29i1.259025.

Article history:
Received: Apri1 28, 2025
Revised: November 2, 2025
Accepted: November 4, 2025
Available online: December 14, 2025

Abstract: This study presents a detailed experimental investigation into the energy and exergy efficiencies of a double-pass solar air heater (SAH) augmented with porous materials. The primary objective was to assess the impact of integrating steel-based hollow square porous elements, featuring porosities of 0.98 and 0.99, on the thermodynamic performance of the SAH under tropical environmental conditions. A prototype SAH with dimensions of 0.75 m × 1.85 m × 0.25 m was developed and evaluated based on empirical data encompassing solar irradiance, air inlet and outlet temperatures, and mass flow rate. The results demonstrate a significant improvement in both energy and exergy efficiencies with the incorporation of porous materials. Notably, the configuration with 0.98 porosity yielded superior results, with energy efficiencies ranging from 6.19% to 9.01% and a peak exergy efficiency of 0.26%. In comparison, the reference system without porous material exhibited lower average energy and exergy efficiencies of 4.98% and 0.11%, respectively. Furthermore, the porous media contributed to enhanced thermal inertia, leading to improved heat retention and a more stable outlet temperature profile under fluctuating solar irradiance. These findings underscore the thermodynamic advantages of utilizing high-porosity materials within a double-pass SAH, emphasizing their potential for efficient thermal energy conversion in agricultural and industrial drying applications, particularly in regions with high solar potential.

Keywords: Solar air heater; porous materials; energy efficiency; exergy efficiency; experimental

1. Introduction

Solar energy constitutes a renewable and environmentally sustainable resource capable of long-term, uninterrupted exploitation. Positioned within the equatorial zone, Thailand possesses substantial solar energy potential. The utilization of solar radiation in the country predominantly follows two main pathways: direct conversion into electrical energy and thermal energy applications. Given Thailand's high solar irradiance levels, deploying solar collectors for thermal processes, particularly in drying and industrial heating applications, presents a highly viable and promising approach. Furthermore, as an agriculturally oriented nation, Thailand's solar energy applications support agricultural processes and enhance energy sustainability. Therefore, the application of solar energy in agriculture predominantly involves its use as a

thermal source. In the industrial sector, solar energy preheats air, reducing conventional energy consumption in thermal processes. In agricultural and industrial contexts, solar energy is frequently integrated as a primary heat source in drying systems to enhance energy efficiency and sustainability [1-3]. The solar collector is the device employed to elevate air temperature for thermal applications. Nevertheless, the deployment of solar energy continues to face challenges, primarily due to the intermittent and variable nature of solar irradiance. Solar energy systems are limited by seasonal and weather-dependent variations in intensity. On average, solar radiation on Earth's surface is approximately 1,000 W/m². The Sun's surface temperature is estimated to be approximately 5778 K, commonly referred to as its effective temperature. This parameter represents the temperature of an ideal blackbody that would radiate the same total energy per unit area as the Sun across the entire electromagnetic spectrum [4-6]. Optimizing solar exposure through angle adjustments aligned with the Sun's trajectory can significantly enhance energy capture. In Thailand, solar radiation averages 4–5 kWh/m²/day, and the use of tracking systems can further increase energy gain by 1.3 to 1.5 times [7,8]. Over the past decades, extensive research efforts have been dedicated to exploring diverse strategies aimed at improving the thermal performance of solar air heaters. Ismail et al. [9] investigated a double-pass solar air heater enhanced with lava rock as a porous medium. Incorporating lava rock improved the system's thermal storage capacity, positioning it as an effective short-term thermal energy collector for solar drying applications. Its presence increased convective heat transfer by enlarging the effective surface area and promoting airflow turbulence. A numerical model based on energy balance equations was developed and solved using MATLAB to assess thermal performance under varying solar radiation and wind conditions. Key parameters included collector dimensions, air mass flow rate, and lava rock volume. The optimal thermal efficiency ranged from 62% to 64% under solar irradiance between 500 and 800 W/m², with a peak efficiency at a flow rate of 0.035 kg/s. An optimal porosity of approximately 89% was identified, balancing thermal performance with pressure drop. The system attained output air temperatures between 41.7°C and 48.3°C, making it suitable for food and agricultural drying. Compared to conventional DPSAH configurations, the lava rock-enhanced system achieved over 17.5% higher outlet temperatures, confirming its potential for improving thermal efficiency. Srivastava et al. [10] conducted an experimental investigation into the thermal performance of a flat plate solar collector and a solar dryer. Their study presented the performance characteristics of the solar collector and solar dryer integrated with a phase change material storage system under quasi-steady-state conditions. The analysis was based on the fundamental energy balance of the system, and a computational model was developed to predict various performance parameters of the solar drying system. The study compared its predictions with theoretical calculations to validate the thermal model. Additionally, optimal values for both solar collector efficiency and dryer efficiency were determined using a genetic algorithm. A comparative assessment was performed among the experimental, theoretical, and optimized efficiency values of the solar collector and dryer. Experimental trials were conducted over multiple days between June 2013 and March 2014 to evaluate the empirical performance of the system. The findings indicated strong agreement between the theoretical, experimental, and optimized efficiency values of the solar collector and dryer, reinforcing the reliability of the proposed model. Jadallah et al. [11] conducted a comprehensive investigation into the performance of a dual-pass hybrid photovoltaic-thermal (PVT) solar cell system designed for drying applications. Their study encompassed both theoretical and experimental analyses, including the design, construction, and modeling of the system to simulate its output. The PVT heat collector extracts hot air, which can be utilized as a heat source for drying processes. Key performance parameters, including temperature distribution, useful heat, electrical power generation, and thermal efficiency, were evaluated using MATLAB, a software specifically developed for this purpose. The findings indicate that the highest outlet fluid temperature achieved was 63°C at a lower mass flow rate of 0.017 kg/s. Furthermore, at a higher mass flow rate, the system exhibited peak electrical, thermal, and overall efficiencies of 12.65%, 56.73%, and 85%, respectively. The maximum electrical and thermal power outputs were recorded at 50.57 W and 389.37 W, respectively. These results demonstrate the system's potential for efficient integration into drying applications, leveraging both electrical and thermal energy outputs. Kumar et al. [12] conducted a comprehensive study on the influence of porous materials on the flow characteristics and temperature distribution within a passive solar air heater. The research examines the impact of flow resistance induced by a porous medium, which

represents agricultural products, at the outlet of a free-convection-based solar air heater. Both experimental and numerical approaches were employed to analyze these effects. The findings provide valuable insights into optimizing the design and efficiency of solar air heaters for agricultural drying applications. Additionally, incorporating porous materials into solar collector absorber plates has been shown to significantly enhance thermal efficiency and stabilize air temperatures, even during periods of low solar radiation [13-16]. Research has demonstrated that combining porous materials with advanced solar collector panels enhances drying performance and energy efficiency [17-20]. Porous materials improve thermal energy retention and gradual release, ensuring stable drying chamber temperatures. Moreover, an experimental study was undertaken to enhance the thermal efficiency of hot air temperature augmentation systems by integrating porous materials. Hwang et al. [21] conducted an extensive investigation focusing on the design and performance assessment of high-efficiency solar air heaters embedded with porous structures. Their work involved the development of a comprehensive theoretical model, which was subsequently validated through experimental testing. The study systematically examined the radiative characteristics of glass covers and porous absorber materials to optimize thermal performance. The experimental outcomes indicated that daily thermal efficiencies consistently surpassed 60%, aligning closely with theoretical estimations. Integrating porous materials significantly enhanced thermal efficiency, with empirical results confirming the precision and practical relevance of the proposed theoretical framework. Hameed et al. [22] conducted an experimental investigation to assess the influence of integrating porous materials, specifically steel wool, on the thermal performance of single-pass solar air heaters. The study involved a comparative analysis between conventional flat absorber plates and those modified with porous media, focusing on key performance parameters such as outlet air temperature and thermal efficiency across different air mass flow rates. Two configurations were examined: a standard setup and one incorporating steel wool positioned above the absorber plate. Experiments were conducted at air mass flow rates of 0.015 and 0.035 kg/s. The findings revealed that the outlet temperature increased by 12.28% and 21.32% at flow rates of 0.015 and 0.035 kg/s, respectively. Furthermore, incorporating porous materials improved thermal efficiency by approximately 10%. These results underscore the effectiveness of porous materials integration in enhancing outlet air temperatures and overall thermal efficiency in solar air heaters. Jalil and Ali [23] conducted an experimental evaluation of the thermal performance of a double-pass solar air heater utilizing stainless steel mesh and steel wool as porous media. The study systematically examined the influence of key porous media properties, including porosity, thermal conductivity, and mass flow rate, on the system's thermal efficiency. The findings demonstrated that including porous materials resulted in a notable enhancement in thermal efficiency compared to configurations without porous media. Specifically, steel wool exhibited a maximum thermal efficiency of 79.82%, while stainless steel mesh achieved 76%. Furthermore, the efficiency improvements associated with steel wool at porosities of 98.75%, 97.5%, and 96.25% were recorded as 6%, 12.6%, and 31.7%, respectively. The results conclusively indicate that porous materials characterized by lower porosity and higher thermal conductivity substantially augment the thermal efficiency of double-pass solar air heaters. Abo-Elfadl et al. [24] investigated the energy, exergy, and economic performance of a novel tubular solar air heater incorporating porous materials. The study systematically assessed the impact of porous media and flow configurations (single-pass and double-pass) on key performance indicators, including energy gain, outlet air temperature, energy, and exergy efficiencies, as well as economic factors such as payback period and overall system cost. An experimental setup was established to compare the performance of tubular and conventional flat-plate solar air heaters under both single and double-pass flow configurations at varying air mass flow rates of 0.075, 0.05, and 0.025 kg/s. The findings demonstrated that integrating porous materials significantly enhanced outlet air temperature. Additionally, the tubular solar air heater with porous media exhibited superior energy, exergy, and economic performance compared to its flat-plate counterpart. Salih et al. [25] conducted an experimental investigation to assess the performance effects of integrating porous media within double-pass solar air heaters operating under natural and forced convection conditions. The study evaluated system efficiency and temperature differentials under consistent winter environmental settings, with the solar air heaters designed using double glass covers. The results demonstrated that double-pass solar air heaters incorporating porous materials achieved notably higher thermal efficiencies than those without, under natural and forced air circulation. The

presence of porous material was found to substantially enhance heat transfer rates and overall system performance, with the improvements particularly pronounced under forced convection conditions. Previous studies have demonstrated that incorporating porous materials into solar air heaters significantly enhances their thermal performance. Consequently, enhancing the thermal efficiency and overall performance of solar air heaters has become a focal point of contemporary research. However, a critical analysis of the existing literature reveals a research gap concerning the integration of porous materials in solar collectors to augment their thermal performance. In response to this gap, the present study investigates the effect of incorporating porous materials, specifically steel hollow square elements, on the absorber plate of a solar collector. The study also examines key influencing parameters and their interdependencies to comprehensively understand their impact on system efficiency. Furthermore, this investigation aims to demonstrate the potential of the proposed configuration in achieving elevated outlet air temperatures while enabling thermal energy storage during periods of low or no solar irradiance, such as cloudy conditions.

2. Materials and Methods

2.1 Experimental setup

This study conducted experimental investigations using a double-pass solar air heater. The solar air heater was constructed with a width of 0.75 m, a length of 1.85 m, and a height of 0.25 m, featuring an absorber plate made of 0.0015 m-thick steel. To enhance thermal efficiency, porous structures were introduced and fabricated from perforated steel sheets with a 0.01 m diameter and a thickness of 0.0012 m. These sheets were precisely cut and assembled into hollow rectangular enclosures with dimensions of 0.05 m × 0.05 m and 0.1 m × 0.1 m, corresponding to porosities of 0.99 and 0.98, respectively. The enclosures extended across the width of the solar collector and were positioned directly above the absorber plate to improve heat absorption and retention. Centrifugal fans are used to introduce air into the solar air heater from the top of the absorber plate, where it flows downward, circulates toward the bottom of the absorber plate, and is subsequently discharged from the solar air heater. The schematic diagram and photographic representations of the solar air heater and porous material are presented in Figures 1 and 2.

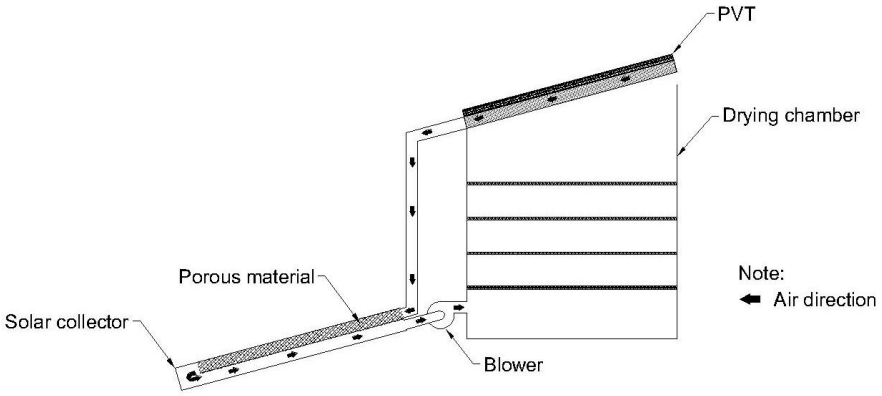

Figure 1. Schematic diagram of the solar air heater.

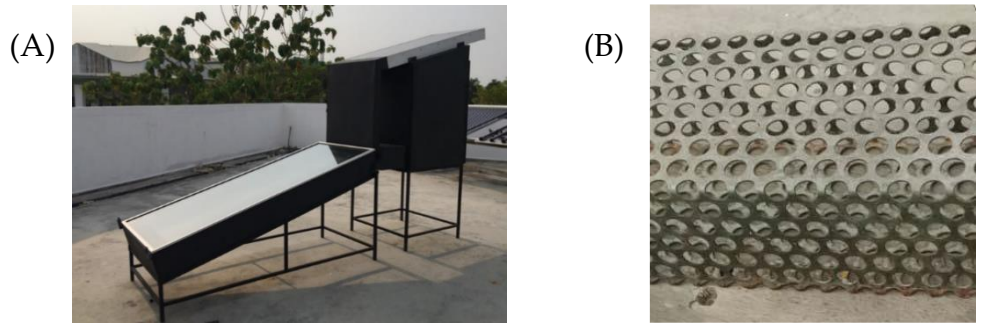

Figure 2. (A) Photograph of the solar air heater, (B) Photograph of porous material.

The experimental evaluation of the solar air heater (SAH) was conducted in Thailand under tropical climatic conditions during clear-sky days on 4th November and 24th December 2024, between 9:00 a.m. and 4:00 p.m., and data were collected over three test runs. The air velocity within the solar air heater was measured using a hot-wire anemometer, featuring a measurement range of 0 to 20 m/s, a tolerance of ±0.03 m/s ±5%, and a resolution of 0.1 m/s. Throughout the experimental procedures, the air velocity was maintained at 0.07 m/s, corresponding to the minimum airflow typically used in solar dryers. Temperature measurements were recorded using K-type thermocouples connected to a data logger, with an accuracy of ±1 °C. The solar irradiation values were recorded using a calibration from the power generation rate of the solar cell compared to a TENMARS solar radiation meter model TM-207 with an accuracy of 5% and a resolution of 1 W/m². Figures 3 and 4 show solar irradiation measurement instruments and calibration results of the solar cell and the solar irradiation meter.

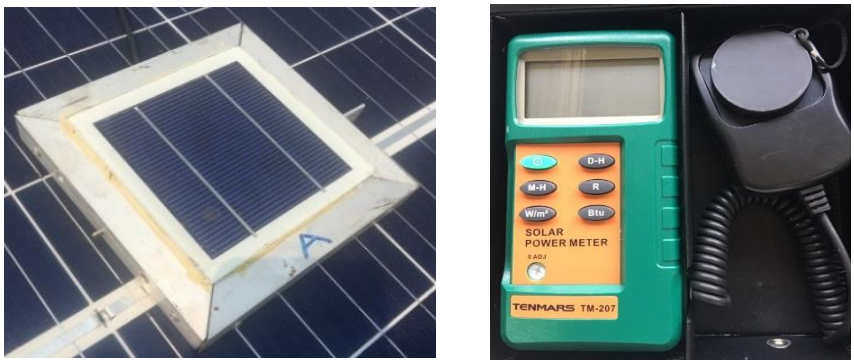

Figure 3. Solar irradiation measurement instruments.

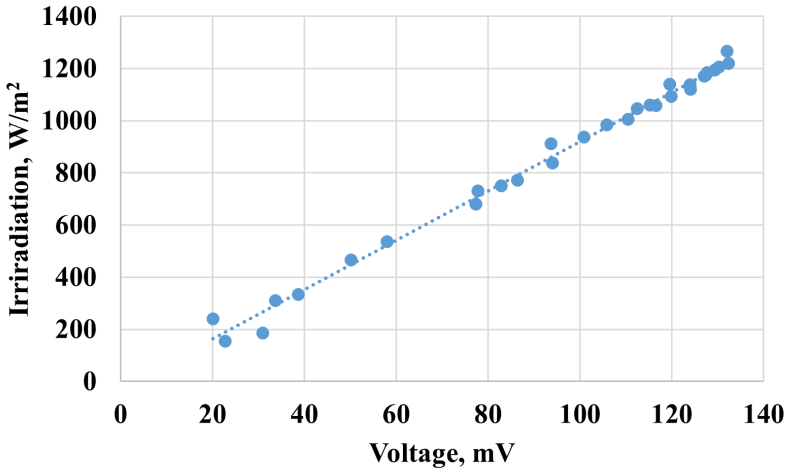

Figure 4. Calibration results for solar cells and a solar irradiance meter.

Based on the calibration results of the solar cell and solar irradiation meter, the relationship can be expressed as Equation (1). The calibration demonstrated a high coefficient of determination ($R^2 = 0.9934$) and was validated for solar irradiance levels within the range of 300–1200 W/m².

$$I = 9.4607V - 27.152 \quad (1)$$

I = solar irradiance (W/m²)
(representing the equivalent solar irradiation measured by calibrated photovoltaic cells)
V = voltage output generated by the solar cell (mV)

Porosity is a fundamental characteristic of porous materials. It represents the proportion of void space relative to the material's total bulk volume. It can be calculated using the following general formula [9]:

$$\phi = \frac{V_v}{V_t} \tag{2}$$

ϕ = porosity of porous materials
V_v = volume of the pore (m^3)
V_t = total (bulk) volume of the material (m^3)

2.2 Analysis

Equation 3 is the fundamental governing equation for determining the useful energy of air through a solar air heater.

$$Q_a = mc_p\Delta T = \rho V c_p \Delta T \tag{3}$$

Q_a = useful heat (kJ)
m = mass flow rate (kg/s)
c_p = specific heat capacity (kJ/kg·K)
ΔT = temperature variation between outlet and inlet (°C)
ρ = air density (kg/m^3)
V = air volume flow rate (m^3/s)

The following equation, equation 4, can calculate the thermal efficiency of 1st law of thermodynamics:

$$\eta_{th} = \frac{Q_a}{I \cdot A_c} \tag{4}$$

Q_a = useful heat (kJ)
I = solar irradiation (W/m^2)
A_c = Solar collector area (m^2).

Exergy denotes the maximum useful work a system can achieve as it progresses toward thermodynamic equilibrium with its environment. In a solar air heater (SAH), exergy analysis is critical for assessing the system's intrinsic thermodynamic performance, extending beyond the conventional first-law energy analysis. The exergy efficiency, grounded in the second law of thermodynamics, can be determined using the following expression in equation 5.

$$\eta_{ex} = \frac{mc_p\left[(T_o - T_i) - T_{amb} ln\left(\frac{T_o}{T_i}\right)\right]}{I \cdot A_c\left(1 - \frac{T_{amb}}{T_{sun}}\right)} = \frac{\rho V c_p\left[(T_o - T_i) - T_{amb} ln\left(\frac{T_o}{T_i}\right)\right]}{I \cdot A_c\left(1 - \frac{T_{amb}}{T_{sun}}\right)} \tag{5}$$

T_{amb} = ambient air temperature (K)
T_o = outlet air temperature (K)
T_i = inlet air temperature (K)
T_{sun} = Sun temperature (K).

2.3 Uncertainty Analysis

Measurement uncertainties were considered for key parameters, including air temperature, velocity, and solar irradiance. The uncertainties associated with the K-type thermocouples, hot-wire anemometer, and solar radiation meter were ±1.0 °C, ±5%, and ±5%, respectively. The combined uncertainty for calculated quantities such as thermal efficiency (η_{th}) and exergy efficiency (η_{ex}) was estimated using the general error propagation formula:

$$\frac{\Delta R}{R} = \sqrt{\left(\frac{\Delta T}{T}\right)^2 + \left(\frac{\Delta I}{I}\right)^2 + \left(\frac{\Delta V}{V}\right)^2} \quad (6)$$

R = calculated result (thermal efficiency, exergy efficiency)
T, I, V = measured parameters (air temperature, solar irradiance, air velocity)
Δ = respective uncertainties

Table 1 shows a summary of the individual uncertainties for each measured parameter. Applying this approach, the combined relative uncertainty for thermal and exergy efficiency was approximately ±7% and ±9%, respectively, under typical experimental conditions.

Table 1. Summarizes the individual uncertainties for each measured parameter.

Measurement	Value (example)	Uncertainty (%)	Instrument
Air temperature (T)	30–50 °C	±1.0 °C (≈±3%)	K-type thermocouple
Solar irradiance (I)	600–900 W/m²	±5%	Solar meter (TM-207)
Air velocity (V)	0–20 m/s	±5%	Hot-wire anemometer

3. Results and Discussion

An experimental analysis was performed without porous materials from 9:00 a.m. to 4:00 p.m. The study provided crucial insights into solar radiation levels and temperature profiles across the solar air heater (SAH). Figure 5 shows the experimental result of SAH without porous materials. Solar radiation values ranged from 572 to 872 W/m², with an average of 717.1 W/m². The inlet air temperature varied between 29°C and 32°C, with a mean temperature of 30.2°C. The outlet temperature fluctuated between 33°C and 48°C, with an average of 40.2°C. The temperature inside SAH ranged from 30°C to 46°C, with an average of 37.5°C. Recorded ambient temperatures ranged from 29°C to 31°C, with a mean value of 29.6°C. Additionally, the temperature of the glass panel ranged from 31°C to 51°C, with an average temperature of 42.1°C. The findings of this investigation are presented in Figure 5, illustrating that the outlet temperature of SAH exhibits significant variation in response to fluctuations in solar irradiance. An increase in solar irradiance corresponds to a rise in outlet temperature. In contrast, reducing irradiance, such as during intermittent cloud cover, dramatically decreases outlet temperature, resulting in continuous dynamic changes.

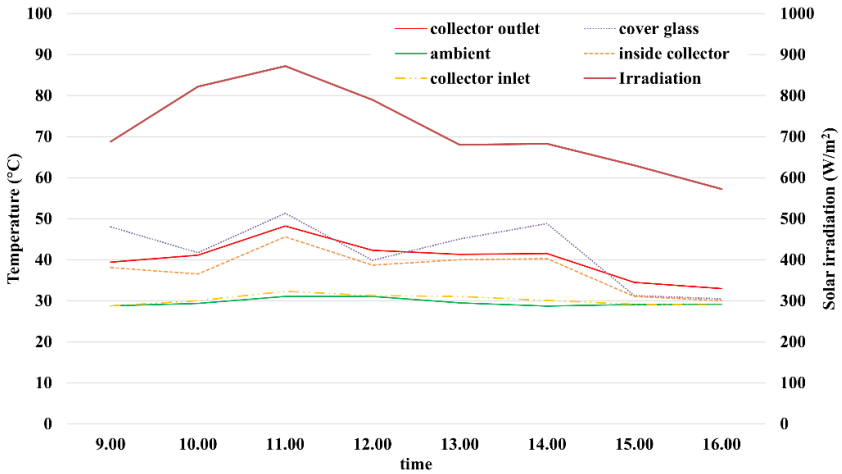

Figure 5. Temperature profile of the SAH without porous material.

Figure 6 shows an experimental result of SAH with porous material with 0.99 porosity. Solar radiation values ranged from 725 to 960 W/m², with an average of 809.8 W/m². The inlet air temperature varied between 27°C and 33°C, with a mean temperature of 30.7°C. The outlet temperature fluctuated between 39°C and 46°C, with an average of 42.5°C. The temperature inside the SAH ranged from 36°C to

42°C, with an average of 39.1°C. Recorded ambient temperatures ranged from 26°C to 33°C, with a mean value of 30.3°C. Additionally, the temperature of the glass panel ranged from 39°C to 49°C, with an average temperature of 43.5°C. The outlet temperature of SAH exhibited minimal variation in response to changes in solar irradiance. An increase in solar intensity generally led to a corresponding rise in outlet temperature. Conversely, a reduction in solar irradiance, such as that caused by intermittent cloud cover, resulted in a modest yet relatively stable decline in outlet temperature throughout the duration of the experimental observation.

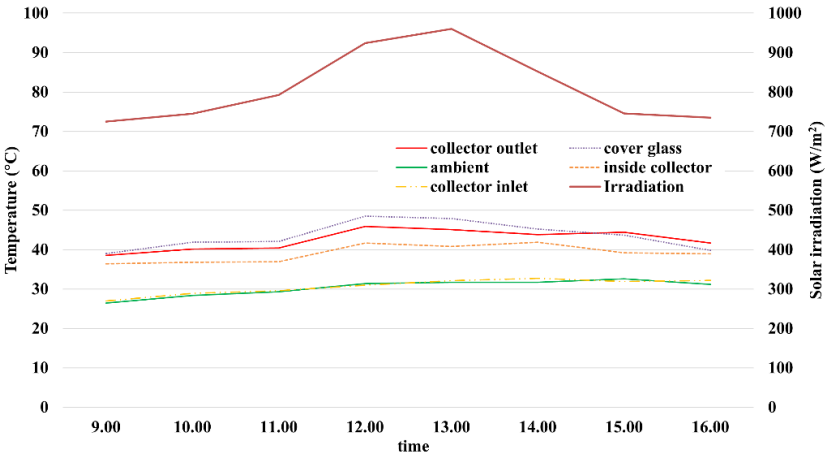

Figure 6. Temperature profile of the SAH with porous material at a porosity of 0.99.

Figure 7 shows an experimental result of SAH with porous material with 0.98 porosity. Solar radiation values ranged from 722 to 877 W/m², with an average of 804.4 W/m². The inlet air temperature varied between 29°C and 34°C, with a mean temperature of 31.1°C. The outlet temperature fluctuated between 44°C and 52°C, with an average of 48.4°C. The temperature inside SAH ranged from 34°C to 47°C, with an average of 38.9°C. Recorded ambient temperatures ranged from 31°C to 35°C, with a mean value of 33.2°C. Additionally, the temperature of the glass panel ranged from 41°C to 54°C, with an average temperature of 48.5°C. The outlet temperature of the solar air heater (SAH) exhibits only minor fluctuations in response to variations in solar irradiance, a behavior consistent with the experimental results incorporating a porous material with a porosity of 0.99. Generally, an increase in solar irradiance leads to a corresponding rise in outlet temperature. In contrast, a reduction in solar irradiance, such as that induced by intermittent cloud cover, causes a slight yet relatively stable decline in the outlet temperature throughout the observation period.

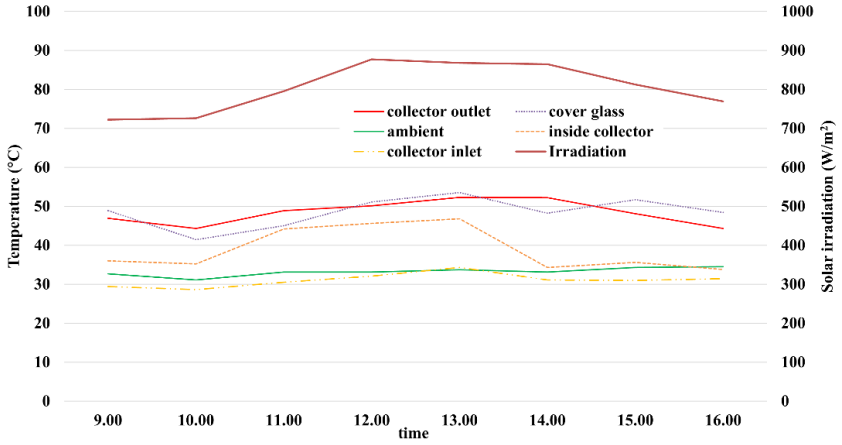

Figure 7. Temperature profile of the SAH with porous material at a porosity of 0.98.

The energy and exergy efficiency of SAH is illustrated in Figures 8 and 9. The experimental analysis of a solar air heater (SAH) incorporating porous materials with porosities of 0.99 and 0.98 revealed significant enhancements in energy and exergy efficiency. Without porous materials, the SAH's energy efficiency ranges from 2.38% to 7.61%, while the exergy efficiency lies between 0.02% and 0.24%. When porous materials with porosity values of 0.98 and 0.99 are introduced, energy and exergy efficiencies improve. Specifically, for porous materials with a porosity of 0.98, the energy efficiency ranges from 6.19% to 9.01%, and the exergy efficiency from 0.07% to 0.26%. In the case of porous materials with a porosity of 0.99, the energy efficiency increases further, ranging from 4.77% to 6.19%, with exergy efficiency values spanning from 0.09% to 0.14%. The highest exergy efficiency is attained with a porous material of 0.98 porosity, reaching approximately 0.2%, particularly evident during midday hours (12:00–13:00). In contrast, the configuration without porous material exhibits a peak around 11:00 hrs (~0.18%), but shows more significant variability throughout the observation period compared to systems incorporating porous materials. The SAH with a porous material of 0.98 porosity benefits from relatively higher and more stable solar irradiance throughout the day, which corresponds to its superior exergy performance. Similarly, regarding the energy efficiency of SAH, the porous material of 0.98 porosity configuration consistently outperforms the others. In contrast, without a porous material, it peaks around 11:00 hrs before experiencing a gradual decline. Incorporating porous material with a 0.99 porosity configuration demonstrates more stable but comparatively lower energy efficiency, averaging approximately 5.40%. These trends align with the exergy performance, whereby the porous material with a 0.98 porosity configuration, subjected to more consistent solar radiation, exhibits enhanced thermal behavior. Post-noon reductions in solar irradiance lead to decreased energy efficiency across all cases. However, incorporating porous material with a 0.98 porosity configuration maintains relatively higher performance due to its improved thermal retention and distribution characteristics. Overall, peak solar irradiance around midday contributes to elevated thermal efficiencies across all configurations, with systems employing porous materials exhibiting prolonged and more stable thermal performance. These results indicate that including porous materials on the absorber plate facilitated the maintenance of elevated outlet air temperatures for extended periods compared to configurations without porous materials. The experimental results demonstrate that incorporating porous materials enhances the thermal efficiency by 8.43% compared to the configuration without porous materials. In agreement with the findings of Hameed et al. [22], the integration of porous media increased the outlet air temperature by 12.28% and 21.32% at mass flow rates of 0.015 kg/s and 0.035 kg/s, respectively. Overall, the incorporation of porous materials contributed to an approximate 10% improvement in thermal efficiency. Moreover, this finding is consistent with Salih et al. [25], who reported that incorporating porous media in a double-pass solar air heater enhanced efficiency to 87% under natural convection and 81% under forced convection, compared to 82% and 67% in the non-porous configuration. The inclusion of porous media significantly improves heat transfer and system performance, particularly under forced convection, with DPSAH-1 recommended for high-temperature applications.

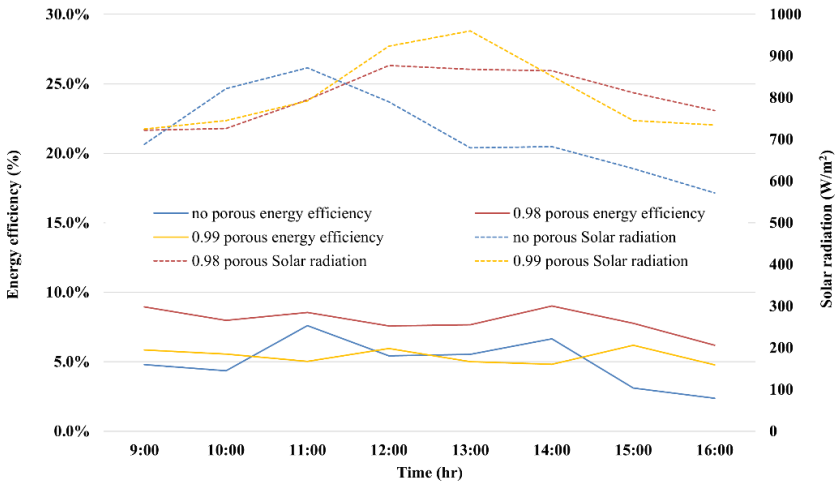

Figure 8. Energy efficiency of the SAH with and without porous material.

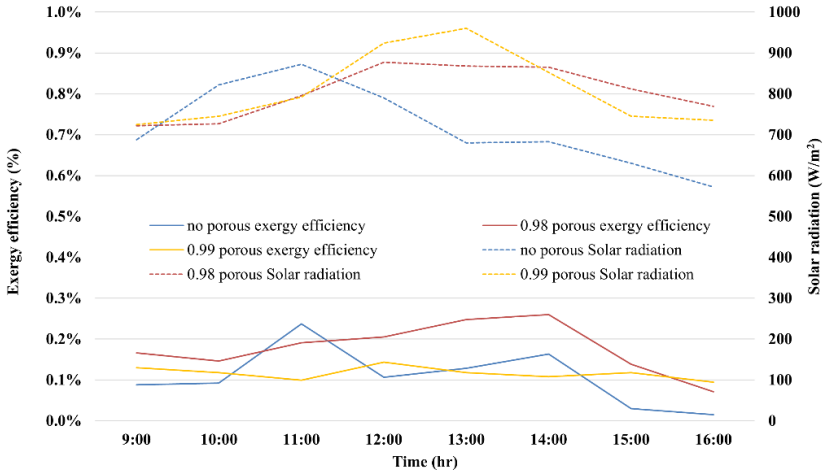

Figure 9. Exergy efficiency of the SAH with and without porous material.

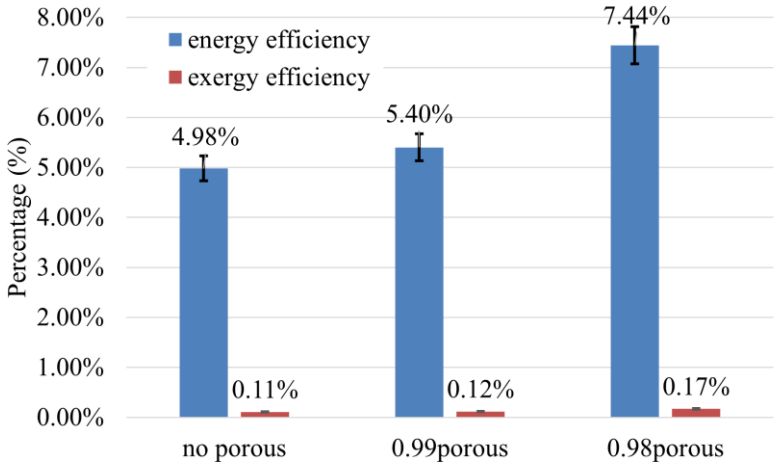

Figure 10. Comparison of the average efficiency of the SAH.

Figure 10 compares the average energy and exergy efficiency of a solar air heater with and without porous materials. Solar air heaters operating without porous materials exhibited an average energy efficiency of 4.89% and an exergy efficiency of 0.11%. In contrast, incorporating porous media with porosities of 0.98 and 0.99 resulted in notable improvements. Specifically, energy efficiency increased to 7.44% and 5.40%, representing approximately 0.5% and 0.08% enhancements, respectively. Correspondingly, exergy efficiencies for these configurations reached 0.17% and 0.12%, indicating a marked improvement in the thermodynamic performance of the SAH with porous materials. Compared to Ismail et al. [9], our results demonstrate a 12% higher energy efficiency under similar conditions. The observed enhancement in system performance can be attributed to improved thermal retention and a more homogeneous distribution of heat within the SAH. The comparative evaluation of the SAH configurations with porous material revealed that the setup without porous material consistently exhibited higher thermal and exergy efficiencies. Specifically, the average thermal efficiency with and without porous material configuration exceeded approximately 0.49%, while the corresponding exergy efficiency improvement was 0.55%. However, it is essential to note that the combined uncertainty margins for thermal and exergy efficiencies were estimated at ±7% and ±9%, respectively. To ensure the robustness of these findings, statistical significance testing was conducted using a Student's *t*-test. The results confirmed that the observed differences between with and without porous material were statistically significant at the 95% confidence level ($p < 0.05$), thereby substantiating the performance

advantage of the 0.98 porosity configuration. These results highlight that, although experimental uncertainties are inherent in solar thermal system testing, the integration of porous material provides a demonstrable improvement in thermodynamic performance compared to one without porous material. This aligns with a well-established characteristic of solar thermal systems, wherein a portion of the input energy becomes unavailable for useful work due to thermodynamic irreversibilities such as viscous dissipation, conductive losses, and suboptimal heat transfer mechanisms. Systems that integrate thermal energy storage or porous material consistently demonstrate superior performance in terms of energy and exergy efficiencies when compared to single-pass configurations or those lacking storage components. The inclusion of these design elements not only increases the total energy harnessed but also improves the thermodynamic quality of energy utilization. While energy efficiency quantifies the amount of energy converted, exergy efficiency assesses the effectiveness of harnessing this energy.

4. Conclusions

This research presents an experimental evaluation of the energy and exergy efficiency of a double-pass solar air heater (SAH) incorporating steel-based porous structures of varying porosities (0.98 and 0.99), under tropical climatic conditions. The objective was to quantify the influence of porous materials integration on energy and exergy efficiencies. The experimental outcomes affirm that integrating porous materials substantially improves the efficiency of the SAH. Notably, the configuration with a porosity of 0.98 exhibited superior results, achieving energy efficiencies ranging from 6.19% to 9.01%, alongside a peak exergy efficiency of 0.26%. These metrics markedly exceed those recorded without porous material configuration, demonstrating average energy and exergy efficiencies of 4.89% and 0.11%, respectively. Including porous materials enhanced thermal retention capabilities and stabilized the outlet air temperature, even under intermittent solar irradiance. These benefits were most pronounced during midday hours, correlating with maximum solar irradiation, thus emphasizing the role of porous structures in increasing thermal inertia and expanding the heat transfer surface area of the solar collector. Furthermore, the lower-porosity configuration (0.98) consistently outperformed the higher-porosity counterpart (0.99), highlighting the efficiency advantages of porous materials with a lower void fraction, which contribute to enhanced thermal storage and improved convective heat transfer. Incorporating porous materials on the absorber surface demonstrably enhances the energy capture and thermodynamic quality of solar air heaters. These findings highlight the suitability of porous-integrated SAH systems for agricultural and industrial drying processes in regions with high solar potential. This work provides a potential pathway for improving SAH designs with porous materials in tropical climates. Future research should investigate the use of alternative porous materials and explore other applications of solar air heaters for various purposes. Furthermore, future studies should investigate the impact of varying wind speeds across different climates, geographic contexts, and seasonal variations.

5. Acknowledgments

The authors thank the Department of Mechanical Engineering, Faculty of Engineering, Ubon Ratchathani University, for the financial support.

Author Contributions: Conceptualization: U. T., and A. N.; Methodology: U. T., A. N., P. S., S. S., and E. B.; Formal analysis and investigation: U. T., A. N., and E. B.; Writing —original draft preparation: E. B.; Writing —review and editing: U. T., and A. N.; Supervision: U. T., Projection administration: E. B., and U. T, All authors have read and agreed to the published version of the manuscript.

Funding: This research was funded by the Department of Mechanical Engineering, Faculty of Engineering, Ubon Ratchathani University.

Conflicts of Interest: The authors declare no conflict of interest.

References

[1] Azis, A.; Waris, A.; Salim, I.; Syafiuddin, M.; Setiawan, E.; Rezkiana, N.; Azizah, A.; Alamsyah, M. Testing the Heat Distribution of Flat Plate Type Solar Collectors for LPG Solar Hybrid Dryers at P4S Bukit Melintang. *BIO Web Conf.* **2024**. https://doi.org/10.1051/bioconf/20249603004

[2] Senthil, R.; Vijayan, G.; Phadtare, G.; Gupta, B. Performance Enhancements of Solar Dryers Using Integrated Thermal Energy Storage: A Review. In *Proceedings* **2021**, 355–362. https://doi.org/10.1007/978-981-15-9678-0_31

[3] Panwar, N.; Kaushik, S.; Kothari, S. State of the Art on Solar Drying Technology: A Review. *Int. J. Renew. Energy Technol.* **2012**, *3*, 107. https://doi.org/10.1504/IJRET.2012.045622

[4] Masana, E.; Jordi, C.; Ribas, I. Effective Temperature Scale and Bolometric Corrections from 2MASS Photometry. *arXiv* **2006**. https://doi.org/10.1051/0004-6361:20054021

[5] Ji, F.; Ji, F.; Dai, X. A New Solution Method for Black-Body Radiation Inversion and the Solar Area-Temperature Distribution. *Sci. China Phys. Mech. Astron.* **2011**, *54*(11), 2097–2102. https://doi.org/10.1007/S11433-011-4514-7

[6] Cugliandolo, L. F. The Effective Temperature. *J. Phys. A* **2011**, *44*(48), 483001. https://doi.org/10.1088/1751-8113/44/48/483001

[7] Nimnuan, P.; Janjai, S. An Approach for Estimating Average Daily Global Solar Radiation from Cloud Cover in Thailand. *Procedia Eng.* **2012**, *32*, 399–406. https://doi.org/10.1016/J.PROENG.2012.01.1285

[8] Waewsak, J.; Chancham, C.; Mani, M.; Gagnon, Y. Estimation of Monthly Mean Daily Global Solar Radiation over Bangkok, Thailand Using Artificial Neural Networks. *Energy Procedia* **2014**, *57*, 1160–1168. https://doi.org/10.1016/J.EGYPRO.2014.10.103

[9] Ismail, A.; Hamid, A.; Ibrahim, A.; Jarimi, H.; Sopian, K. Performance Analysis of a Double Pass Solar Air Thermal Collector with Porous Media Using Lava Rock. *Energies* **2022**. https://doi.org/10.3390/en15030905

[10] Srivastava, A.; Shukla, S.; Singh, U. Thermal Performance Analysis of Flat Plate Solar Collector and Solar Dryer of Indirect Solar Drying System. *J. Therm. Eng.* **2016**, *2*, 21–31.

[11] Jadallah, A.; Alsaadi, M.; Hussien, S. The Hybrid Photovoltaic-Thermal Double-Pass Solar System for Drying Applications. *IOP Conf. Ser.: Mater. Sci. Eng.* **2020**, *765*. https://doi.org/10.1088/1757-899X/765/1/012024

[12] Kumar, D.; Premachandran, B. Investigation of the Effect of Porous Material on the Flow and Temperature Patterns of a Passive Solar Air Heater. *J. Sol. Energy Eng.* **2020**, *142*. https://doi.org/10.1115/1.4046632

[13] Nima, F. J.; Steffan, T. L. Performance Improvement of a Solar Air Heater by Covering the Absorber Plate with Porous Material. *Energy* **2020**, *190*, 116437

[14] Singh, S.; Dhiman, P. Thermal Performance of Double Pass Packed Bed Solar Air Heaters—A Comprehensive Review. *Renewable Sustainable Energy Rev.* **2016**, *53*, 1010–1031.

[15] Dissa, A. O.; Ouoba, S.; Bathiebo, D.; Koulidiati, J. A Study of a Solar Air Collector with a Mixed "Porous" and "Non-Porous" Composite Absorber. *Sol. Energy* **2016**, *129*, 156–174.

[16] Murali, G.; Reddy, K. R. K.; Kumar, M. T. S.; Manikanta, J. S.; Reddy, V. N. K. Performance of Solar Aluminium Can Air Heater Using Sensible Heat Storage. *Mater. Today Proc.* **2020**, *21*(1), 169–174.

[17] Vijayan, S.; Arjunan, T. V.; Kumar, A.; Matheswaran, M. M. Experimental and Thermal Performance Investigations on Sensible Storage Based Solar Air Heater. *J. Energy Storage* **2020**, *31*, 101620.

[18] Bayrak, F.; Oztop, H. F.; Hepbasli, A. Energy and Exergy Analyses of Porous Baffles Inserted Solar Heaters for Building Applications. *Energy Build.* **2013**, *57*, 338–345.

[19] Ahmad, O. K.; Mohammed, Z. A. Influence of Porous Media on the Performance of Hybrid PV/Thermal Collector. *Renewable Energy* **2017**, *112*, 378–387.

[20] Hao, W.; Lu, Y.; Lai, Y.; Yu, H.; Lyu, M. Research on Operation Strategy and Performance Prediction of Flat Plate Solar Collector with Dual-Function for Drying Agricultural Products. *Renewable Energy* **2018**, *127*, 685–696.

[21] Hwang, Y.; Park, S. A Theoretical and Experimental Study for the Design of Solar Air Heaters Using Porous Material. *Trans. Korean Soc. Mech. Eng. B* **1996**, *20*, 336–345. https://doi.org/10.22634/KSME-B.1996.20.1.336

[22] Hameed, A.; Mohammed, A.; Hussain, E. Experimental Study of the Effect of Porous Media on the Performance of Single-Pass Solar Air Heater. *J. Adv. Res. Fluid Mech. Therm. Sci.* **2024**. https://doi.org/10.37934/arfmts.121.1.2738

[23] Jalil, J.; Ali, S. Thermal Investigations of Double Pass Solar Air Heater with Two Types of Porous Media of Different Thermal Conductivity. *Eng. Technol. J.* **2021**. https://doi.org/10.30684/ETJ.V39I1A.1704

[24] Abo-Elfadl, S.; Yousef, M.; El-Dosoky, M.; Hassan, H. Energy, Exergy, and Economic Analysis of Tubular Solar Air Heater with Porous Material: An Experimental Study. *Appl. Therm. Eng.* **2021**, *196*, 117294. https://doi.org/10.1016/J.APPLTHERMALENG.2021.117294

[25] Salih, M.; Alomar, O.; Yassien, H. Impacts of Adding Porous Media on Performance of Double-Pass Solar Air Heater under Natural and Forced Air Circulation Processes. *Int. J. Mech. Sci.* **2021**, *210*, 106738. https://doi.org/10.1016/J.IJMECSCI.2021.106738